

Zeitschrift: IABSE reports of the working commissions = Rapports des commissions de travail AIPC = IVBH Berichte der Arbeitskommissionen

Band: 34 (1981)

Artikel: Inelastic analysis of reinforced concrete shear wall structures: material modelling of reinforced concrete

Autor: Shirai, Nobuaki / Sato, Toshio

DOI: <https://doi.org/10.5169/seals-26888>

Nutzungsbedingungen

Die ETH-Bibliothek ist die Anbieterin der digitalisierten Zeitschriften. Sie besitzt keine Urheberrechte an den Zeitschriften und ist nicht verantwortlich für deren Inhalte. Die Rechte liegen in der Regel bei den Herausgebern beziehungsweise den externen Rechteinhabern. [Siehe Rechtliche Hinweise.](#)

Conditions d'utilisation

L'ETH Library est le fournisseur des revues numérisées. Elle ne détient aucun droit d'auteur sur les revues et n'est pas responsable de leur contenu. En règle générale, les droits sont détenus par les éditeurs ou les détenteurs de droits externes. [Voir Informations légales.](#)

Terms of use

The ETH Library is the provider of the digitised journals. It does not own any copyrights to the journals and is not responsible for their content. The rights usually lie with the publishers or the external rights holders. [See Legal notice.](#)

Download PDF: 30.03.2025

ETH-Bibliothek Zürich, E-Periodica, <https://www.e-periodica.ch>

Inelastic Analysis of Reinforced Concrete Shear Wall Structures - Material Modelling of Reinforced Concrete -

Analyse inélastique de la structure asismique des refends en béton armé - Un essai pour obtenir la formule modèle mathématique pour le béton armé -

Inelastische Berechnung von erdbebenfesten Stahlbetonwandkonstruktionen - Modellierung von Stahlbetonmaterialien -

NOBUAKI SHIRAI

Assistant

Department of Architecture, College of Science and Technology, Nihon University, Tokyo, Japan

TOSHIO SATO

Professor

SUMMARY

A finite element formulation capable of clarifying inelastic behavior of reinforced concrete shear wall structures is presented. Inelastic effects such as tensile cracking of concrete, nonlinear stress-strain response of concrete and steel, bond between steel and concrete, aggregate interlock between cracked concrete surfaces and dowel action of reinforcing bars are considered and particular attention is given to a constitutive modelling of these effects which have an important effect upon hysteresis characteristics of reinforced concrete structures. Finally, an incremental self-correcting approach used as a numerical procedure is briefly explained.

RÉSUMÉ

On présente une formule par la méthode des éléments finis capable d'éclairer le comportement inélastique de la structure asismique des refends en béton armé. Compte tenu des effets inélastiques tels que de la fissuration dans le béton due à la traction, de la contrainte non-linéaire et de la réponse de déformation du béton et de l'acier, de l'adhérence entre l'acier et l'armature, de l'effet d'engrènement des faces en béton fissurées et de l'effet goujon, plus particulièrement on a essayé d'obtenir la formule modèle mathématique de constitution desdits effets qui donnent une grande influence sur les caractéristiques d'hystérésis des structures en béton armé. Finalement, on explique en bref le mode d'accès auto-correction incrémental employé comme un procédé numérique.

ZUSAMMENFASSUNG

Es wird eine Formel nach der Methode der finiten Elemente zur Klärung des inelastischen Verhaltens von erdbebenfesten Stahlbetonwandkonstruktionen präsentiert. Es werden inelastische Effekte wie Zugrissbildung im Beton, nichtlineare Spannungsdehnungslinie von Beton und Stahl, Verbund zwischen Stahl und Beton, Rissverzahnung zwischen Betonrissoberflächen, Dübelwirkung des Armierungsstahls betrachtet. Der Modellierung dieser Effekte, die eine wichtige Auswirkung auf die Hysteresecharakteristiken von Stahlbetonkonstruktionen haben, wird besondere Aufmerksamkeit gewidmet. Abschliessend wird kurz eine inkrementelle, selbstkorrigierende Methode erläutert, die als numerische Analyseverfahren verwendet wurde.



1. INTRODUCTION

The reinforced concrete shear structure is a structural system being composed of columns, beams and wall panels and is the most efficient earthquake resistant element. Therefore, it is necessary for investigating inelastic behaviors of reinforced concrete shear wall structures subjected to cyclic loads such as seismic forces to consider all sorts of inelastic effects including cyclic behaviors. Attempts to model inelastic effects have been carried out by many investigators so far, but it is felt that simple and effective models for a finite element formulation have not been proposed yet.

The inelastic effects included in this paper are 1) brittle fracture of concrete (tensile cracking), 2) nonlinear stress-strain response of concrete and steel, 3) bond between concrete and reinforcing bar, 4) aggregate interlock and 5) dowel action. Particularly, the bond model based upon a new concept of bond behaviors and the modelling of aggregate interlock and dowel action evaluated as equivalent shear moduli by introducing crack spacing and width are described in detail.

An incremental initial stress approach or an incremental self-correcting approach which is able to minimize computational time is used as a numerical procedure and here the latter approach, which has not been applied materially nonlinear problems, is briefly explained.

2. MATERIAL IDEALIZATION

Reinforced Concrete is a composite material being made of concrete and steel, and mechanical properties of each component material are idealized as follows.

2.1 Concrete

Uncracked concrete is assumed as a homogeneous isotropic material, and on the other hand cracked concrete is considered to be anisotropic and capable of resisting normal stress parallel to average crack direction.

The uniaxial stress-strain relationship for uncracked concrete is assumed to be elasto-plastic of tri-linear type including strain-softening with a negative slope in compression, and elastic up until to the tensile strength and thereafter concrete changes to a brittle material as shown in Fig.1. In order to simulate compressive behaviors, the yield criterion for plasticity in compression is assumed of either the Von-Mises's formula[1] or the Drucker-Prager's formula[1] and associated flow rule(see Section 3.1),

$$F = A_1 \cdot \sigma_m + A_2 \cdot \bar{\sigma} = A_3 \quad \text{----- (2.1)}$$

where $\sigma_m = (\sigma_x + \sigma_y + \sigma_z)/3$; $\bar{\sigma} = [(s_x^2 + s_y^2 + s_z^2)/2 + \tau_{xy}^2 + \tau_{yz}^2 + \tau_{zx}^2]^{1/2}$; $\sigma_x, \sigma_y, \sigma_z, \tau_{xy}, \tau_{yz}, \tau_{zx}$: the stress components in the orthogonal coordinates X, Y and Z; s_x, s_y, s_z : the deviatoric stresses of $\sigma_x, \sigma_y, \sigma_z$ and the coefficients A_1, A_2 and A_3 are defined in Table 1.

The fracture criterion of Mohr-Coulomb[1] is applied to tensile failure in order to take a reduction of tensile strength due to lateral compressive stresses into consideration,

$$F = (f_c - f_t)(\sigma_m - \bar{\sigma} \sin \phi / \sqrt{3}) / (f_c + f_t) + \bar{\sigma} \cos \phi - f_c f_t / (f_c + f_t) = 0 \quad \text{----- (2.2)}$$

where $\phi = \frac{1}{3} \sin^{-1}[-3\sqrt{3} J_3 / 2\bar{\sigma}^3]$ with $-\pi/6 \leq \phi \leq \pi/6$; $J_3 = s_x s_y s_z + 2\tau_{xy} \tau_{yz} \tau_{zx} - s_x \tau_{yz}^2 - s_y \tau_{zx}^2 - s_z \tau_{xy}^2$; f_c : the uniaxial compressive strength; and f_t : the uniaxial tensile

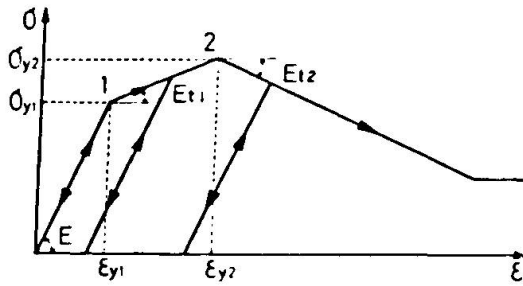


Fig.1 Uniaxial Stress-Strain Relationship for Concrete

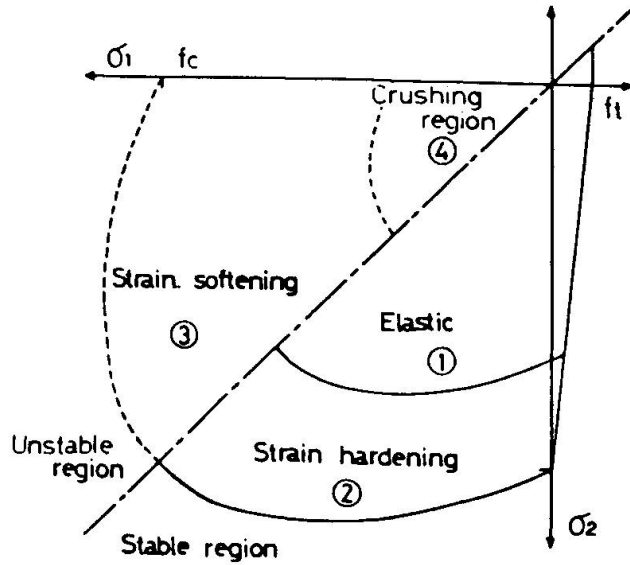


Fig.2 Assumed Fracture and Yield Surfaces of Concrete

IDENTIFICATION # OF CRACK STATES (CPS)	CRACK PATTERNS	DESCRIPTIONS
0		UNCRACKED CONCRETE
1		CONCRETE CRACKED IN ONE DIRECTION
2		FIRST SET OF CRACKS CLOSED
3		FIRST SET OF CRACKS CLOSED SECOND SET OF CRACKS FORMED
4		BOTH SET OF CRACKS CLOSED
5		FIRST SET OF CRACKS OPENED SECOND SET OF CRACKS CLOSED
6		BOTH SET OF CRACKS OPENED

Fig.3 Assumed Cracking Modes

Table 1. Coefficients for Yield Criteria

Yield Criterion	A ₁	A ₂	A ₃
Von - Mises	0	$\sqrt{3}$	$ \gamma(k) $
Drucker - Prager	3c	1	K

where $\alpha = 2\sin\theta/\sqrt{3(3-\sin\theta)}$; $K = 6C\cos\theta/\sqrt{3(3-\sin\theta)}$; $\gamma(k)$: the critical points of uniaxial stress on the trilinear curve and $k = 1, 2$ and 3 ; θ : the angle of friction ; and C : the cohesion.

strength. Fig.2 shows the assumed fracture and yield surfaces in the two-dimensional principal stress plane. The direction of concrete cracks is defined to be perpendicular to principal tensile stress in uncracked concrete just prior to crack formation. In order to be able to pursue behaviors under cyclic loading excursions, six different cracking modes[2] representing the opening and closing of cracks are considered in the present study as shown in Fig.3.

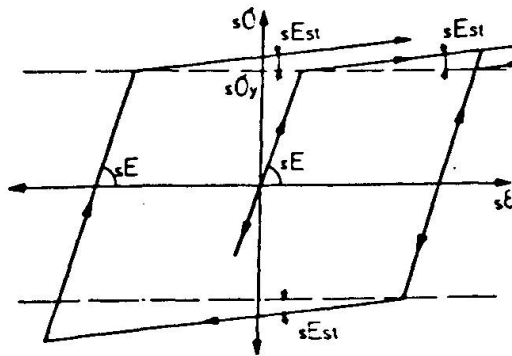
2.2 Steel Reinforcement

The reinforcing bar is regarded as one-dimensional continuous medium in which the area of reinforcing bar distributes uniformly within any concrete element and therefore it is in uniaxial stress state. The stress-strain relationship for reinforcing bar is assumed to be elasto-plastic of bi-linear type with the strain-hardening effect as shown in Fig.4.

The subscripts of σ , E , etc. in the left hand side shall indicate the corresponding materials, and the subscript s is used for steel and c for concrete is omitted in this paper.



Fig.4 Stress-Strain Relationship for Reinforcing Bar



3. MATERIAL STIFFNESS FORMULATION

The material stiffness for reinforced concrete is assumed to be obtained by a linear superposition of component stiffnesses of concrete, reinforcing bar, bond, aggregate interlock and dowel action to be described below.

3.1 Concrete

The material stiffness for elastic uncracked concrete shall follow Hooke's Law for plane stress in an isotropic material. The relation between the incremental stress $\Delta\{\sigma\}$ and the incremental strain $\Delta\{\epsilon\}$ for plastic uncracked concrete was derived on the basis of the Theory of Plasticity along with the yield conditions defined in Eq. (2.1) and associated flow rule [3],

$$\Delta\{\sigma\} = ([D]_e - [D]_p)\Delta\{\epsilon\} = [D]_{ep} \Delta\{\epsilon\} \quad \text{----- (3.1)}$$

where $[D]_e$: the elastic matrix for concrete; $[D]_{ep}$: the elasto-plastic matrix and the plastic matrix $[D]_p$ for plane stress is defined as follows,

$$[D]_p = \frac{E^2}{(1 - \nu^2)^2} \cdot \frac{1}{H' + \bar{\beta}} \begin{bmatrix} d_{11} & d_{12} & d_{13} \\ & d_{22} & d_{23} \\ \text{SYM.} & & d_{33} \end{bmatrix} \quad \text{----- (3.2)}$$

$$\bar{\beta} = E[2A_1^2/9(1 - \nu) + \sigma_m A_1 A_2 / 3(1 - \nu)\bar{\sigma} + \{\sigma_m^3 + 2(1 - \nu)J_3\}A_2^2 / 4\bar{\sigma}^2 \sigma_m (1 - \nu^2)]$$

$$d_{11} = D_1^2, \quad d_{22} = D_2^2, \quad d_{33} = D_3^2, \quad d_{12} = D_1 D_2, \quad d_{13} = D_1 D_3, \quad d_{23} = D_2 D_3,$$

$$D_1 = (1 + \nu)A_1/3 + (S_x + \nu S_y)A_2/2\bar{\sigma}, \quad D_2 = (1 + \nu)A_1/3 + (\nu S_x + S_y)A_2/2\bar{\sigma},$$

$$D_3 = (1 - \nu)\tau_{xy}A_2/2\bar{\sigma}$$

where E : the initial Young's modulus ; ν : the Poisson's ratio ; $H' = \Delta Y / \Delta \epsilon_p$ for the Von-Mises's formula and $(1 - \sqrt{3}\alpha)^2 \Delta Y / \Delta \epsilon_p$ for the Drucker-Prager's formula ; ΔY : the increment of uniaxial yield stress ; and $\Delta \epsilon_p$: the increment of uniaxial plastic strain.

Cracked concrete is subjected to the normal stress σ_u parallel to crack directions and thus the uniaxial stress-strain relation in the U-direction, as indi-

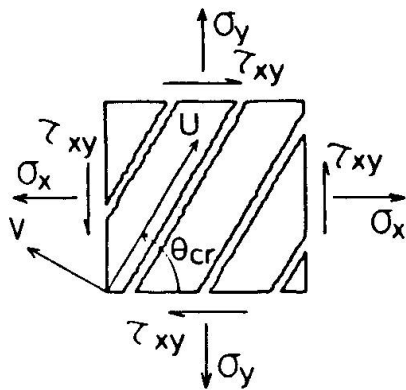


Fig.5 Idealization for Cracked Concrete Element

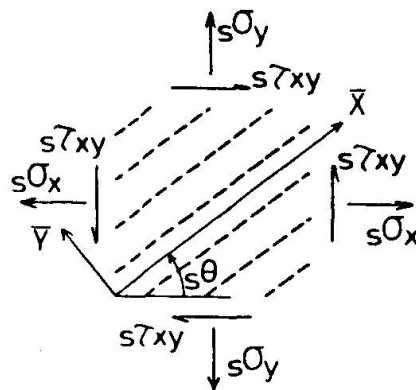


Fig.6 Idealization for Steel Element

cated in Fig.5, is written as follows,

$$\sigma_u = E\epsilon_u \quad \text{with} \quad Y(1) \leq \sigma_u \leq f_t \quad \text{----- (3.3)}$$

If the crack direction makes an angle of θ_{cr} with the X-axis, the stiffness matrix in the local coordinates U,V is converted into that in the global coordinates X,Y by using a appropriate transformation[2],

$$\{\sigma_x\} = [D]_{cr} \{\epsilon_x\} \quad \text{----- (3.4)}$$

in which $\{\sigma_x\} = \{\sigma_x, \sigma_y, \tau_{xy}\}^T$ $\{\epsilon_x\} = \{\epsilon_x, \epsilon_y, \gamma_{xy}\}^T$ and

$$[D]_{cr} = E \begin{pmatrix} \cos^4 \theta_{cr} & \cos^2 \theta_{cr} \sin^2 \theta_{cr} & \cos^3 \theta_{cr} \sin \theta_{cr} \\ & \sin^4 \theta_{cr} & \cos \theta_{cr} \sin^3 \theta_{cr} \\ \text{SYM.} & & \cos^2 \theta_{cr} \sin^2 \theta_{cr} \end{pmatrix} \quad \text{----- (3.5)}$$

The stiffness formulation for cracked concrete in the plastic range ($\sigma_u \leq Y(k)$, where $k = 1, 2$ and 3) is to be done in the same way as the case for elastic cracked concrete ($Y(1) \leq \sigma_u \leq f_t$) by using the tangential moduli E_{t1} and E_{t2} on the uniaxial stress-strain curve corresponding to the strain induced in the crack direction instead of E in Eq.(3.5).

3.2 Steel Reinforcement

Since the reinforcing bar is one-dimensional element, a derivation of the elastic stiffness matrix for reinforcing bar inclined by an angle of $s\theta$ with the X-axis is similar to the case of cracked concrete. The stress-strain relation for reinforcing bar in the \bar{X} -direction, as indicated in Fig.6, is written as follows by assuming the compatibility of deformation,

$$s\sigma_{\bar{x}} = p_{\bar{x}} \cdot sE\epsilon_{\bar{x}} \quad \text{with} \quad -s\sigma_y \leq s\sigma_{\bar{x}} \leq s\sigma_x \quad \text{----- (3.6)}$$

$$p_{\bar{x}} = sA_{\bar{x}}/A \quad \text{----- (3.7)}$$

where sE : the Young's modulus of steel ; $sA_{\bar{x}}$: the area of one bar reinforced in the \bar{X} -direction ; A : the cross sectional area of concrete between reinforcing bars ; and hereafter the subscript s shall indicate steel.

The stiffness matrix of Eq.(3.6) in the global coordinates X,Y takes the following form[2],



$$\{\sigma_x\} = {}_s[D]_e \{\epsilon_x\} \quad \text{----- (3.8)}$$

in which

$${}_s[D]_e = p_{\bar{x}} \cdot {}_sE \begin{pmatrix} \cos^4_s \theta & \cos^2_s \theta \sin^2_s \theta & \cos^3_s \theta \sin_s \theta \\ & \sin^4_s \theta & \cos_s \theta \sin^3_s \theta \\ \text{SYM.} & & \cos^2_s \theta \sin^2_s \theta \end{pmatrix} \quad \text{----- (3.9)}$$

The stiffness formulation for reinforcing bar in the plastic range is to be done in the same way as the case for reinforcing bar in the elastic range by using the tangential Young's modulus ${}_sE_{st}$ on the stress-strain curve corresponding to the strain instead of ${}_sE$ in Eq. (3.9).

3.3 Bond between Concrete and Steel Reinforcement

It has been already known that bond between concrete and reinforcing bar after crack formation gives some resistance to concrete (tension stiffening effect) and its resistance gradually deteriorates with an increase in number of cracks, that is, an increase of strain as shown in Fig.7 [4 and 5].

Referring to experimental results on tensile bond tests [4 and 5], bond effect was replaced by the equivalent stress which indicates the nominal concrete stress, without idealizing it into the discrete element such as the linkage element, and the equivalent stress due to bond is modelled as shown in Fig.8.

It is assumed that the equivalent stress under monotonic loading is represented by the 3rd orders of polynomial function,

$$\left. \begin{aligned} \sigma_{\bar{x},eq} &= f_t \cdot (a_0 + a_1 X + a_2 X^2 + a_3 X^3) \\ \text{with } 0 \leq \sigma_{\bar{x},eq} \leq f_t, \quad \epsilon_{cr} \leq \epsilon_{\bar{x}} \leq \epsilon_{Bu} \quad \text{and} \\ X &= (\epsilon_{\bar{x}} - \epsilon_{cr}) / (\epsilon_{Bu} - \epsilon_{cr}) \end{aligned} \right\} \quad \text{----- (3.10)}$$

where $\sigma_{\bar{x},eq}$: the equivalent stress (kg/cm²) of concrete in the reinforcing direction \bar{X} and the subscript eq indicates an equivalence to the stress σ , τ , etc.; $\epsilon_{\bar{x}}$ (or ${}_s\epsilon_{\bar{x}}$): the average strain of concrete (or reinforcing bar) in the \bar{X} -direction; ϵ_{cr} : the cracking strain; ϵ_{Bu} : the strain at which bond over the element length disappears; and the coefficients a_0 , a_1 , a_2 and a_3 are 1.0, -2.748, 2.654 and -0.906 respectively.

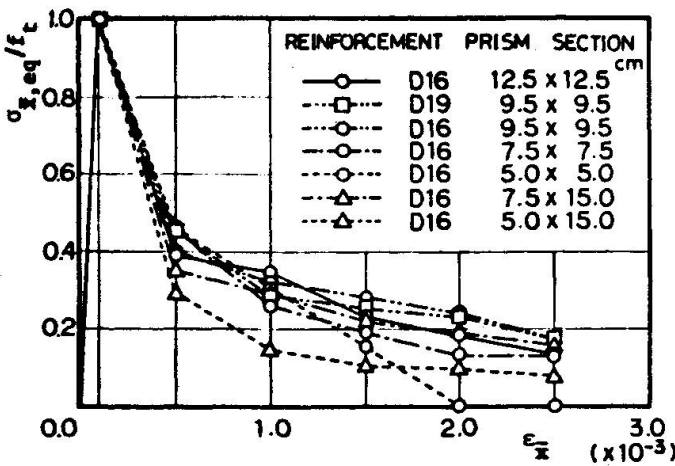


Fig.7 Experimental Equivalent Stress-Average Strain Relation

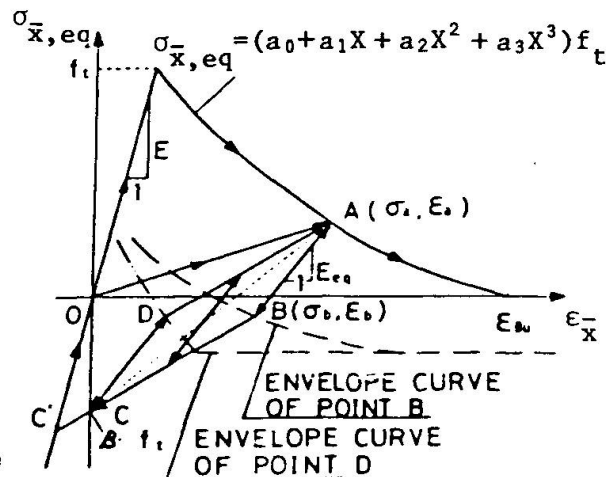


Fig.8 Modelling for Equivalent Stress-Average Strain Relation

Furthermore, the hysteresis for unloading from an arbitrary point A on the curve of Eq.(3.10) was assumed on the basis of a line AC connecting a point A(σ_a, ϵ_a) and a point C($\beta f_t, 0$) on the zero-strain axis as follows,

.for region AB ($\sigma_b \leq \sigma_{\bar{x},eq} \leq \sigma_a$)

$$\sigma_{\bar{x},eq} = E_{eq}(\epsilon_{\bar{x}} - \epsilon_a) + \sigma_a, \quad E_{eq} = \alpha E, \quad \alpha = (\sigma_a + f_t) / E\epsilon_a \quad \text{----- (3.11)}$$

where E_{eq} : the equivalent Young's modulus(kg/cm²) and the equivalent stress σ_b of the point B is set equal to an average of σ_a and σ_c .

.for region BC ($\beta f_t \leq \sigma_{\bar{x},eq} \leq \sigma_b$)

$$\begin{aligned} \sigma_{\bar{x},eq} &= E_{eq} \cdot \epsilon_{\bar{x}} + \beta f_t, & E_{eq} &= (\sigma_a - \beta f_t) / 2\epsilon_b \\ \epsilon_b &= (\beta f_t - \sigma_a) / 2\alpha E + \epsilon_a, & \beta &= -0.5 \end{aligned} \quad \text{----- (3.12)}$$

Nextly, the hysteresis for reloading from a point C or C', where C' is an arbitrary point in the compression range, takes either a path(C→D→A) before the closing of cracks or a path(C'→O→A) after the closing of cracks,

.for region CD ($\beta f_t \leq \sigma_{\bar{x},eq} \leq \sigma_d$)

$$\sigma_{\bar{x},eq} = E_{eq} \epsilon_{\bar{x}} + \beta f_t, \quad E_{eq} = \alpha E \quad \text{----- (3.13)}$$

where the equivalent stress σ_d of a point D is set equal to an average of σ_a and σ_c .

.for region DA ($\sigma_d \leq \sigma_{\bar{x},eq} \leq \sigma_a$)

$$\sigma_{\bar{x},eq} = E_{eq}(\epsilon_{\bar{x}} - \epsilon_a) + \sigma_a, \quad E_{eq} = (\sigma_a - \beta f_t) / 2\epsilon_b \quad \text{----- (3.14)}$$

.for region OA ($0 \leq \sigma_{\bar{x},eq} \leq \sigma_a$)

$$\sigma_{\bar{x},eq} = E_{eq} \epsilon_{\bar{x}}, \quad E_{eq} = \sigma_a / \epsilon_a \quad \text{----- (3.15)}$$

The equivalent stress $\sigma_{\bar{x},eq}$ defined in the above is converted into the stresses $\{\sigma_{\bar{x},eq}, \sigma_{\bar{y},eq}, \tau_{\bar{x}\bar{y},eq}\}$ in the orthogonal coordinates X,Y as follows,

$$\begin{Bmatrix} \sigma_{x,eq} \\ \sigma_{y,eq} \\ \sigma_{xy,eq} \end{Bmatrix} = \begin{bmatrix} \cos^2 \theta & \sin^2 \theta & -2\cos \theta \sin \theta \\ \sin^2 \theta & \cos^2 \theta & 2\cos \theta \sin \theta \\ \cos \theta \sin \theta & -\cos \theta \sin \theta & \cos^2 \theta - \sin^2 \theta \end{bmatrix} \begin{Bmatrix} \sigma_{\bar{x},eq} \\ 0 \\ 0 \end{Bmatrix} \quad \text{---- (3.16)}$$

3.4 Equivalent Shear Stiffness due to Aggregate Interlock

In order to evaluate the shear stress induced along cracked surfaces of concrete due to aggregate interlock after crack formation, Paulay et al.[6] conducted the test on aggregate interlock whose variable factors were concrete strength and crack width, and proposed the shear stress-relative displacement relation. However, since their predicting equation gives a rather high evaluation, it is modified to the following,

$$\tau_{uv,eq1} = (0.141/W - 1.0)(1.526\sqrt{f_c} - 7.365)(\delta_s - 0.0436W) \quad \text{----- (3.17)}$$

where $\tau_{uv,eq1}$: the shear stress acting along cracked surfaces of concrete(kg/cm²) ; W : the crack width(cm) ; δ_s : the relative displacement across cracked surfaces

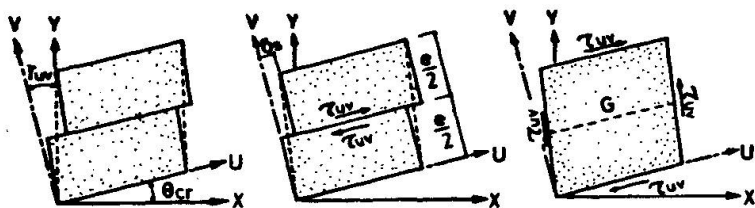


Fig. 9 Assumed Shear Strain for Cracked Concrete

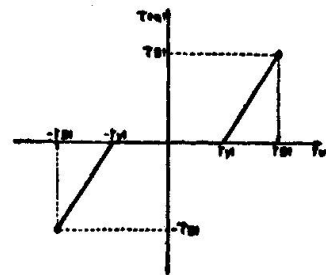


Fig. 10 Assumed Equivalent Shear Stress-Strain Relation of Aggregate Interlock for Constant Crack Spacing and Width

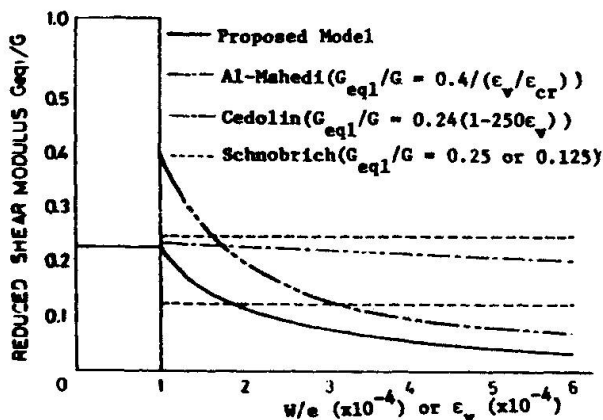


Fig. 11 Shear Stiffness Reduction in Cracked Concrete

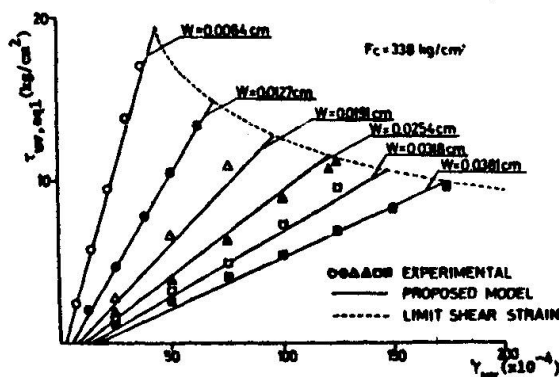


Fig. 12 Comparison between Assumed and Observed Equivalent Shear Stress-Shear Strain Relation

(cm) ; and the subscript s in the right hand side indicates slip. The strain of cracked concrete γ_{uv} is considered to be a sum of the elastic shear strain and the shear strain due to the relative displacement as shown in Fig. 9,

$$\gamma_{uv} = \tau_{uv}/G + \delta_s/e \quad \text{-----} \quad (3.18)$$

where G : the elastic shear modulus(kg/cm^2) ; τ_{uv} : the elastic shear stress in the local coordinates $U, V(\text{kg}/\text{cm}^2)$; and e : the crack spacing(cm). Assuming that the first term in Eq.(3.18) can be negligible as compared with the second term, then Eq.(3.18) can be reduced to,

$$\gamma_{uv} = \delta_s/e \quad \text{with} \quad \gamma_{y1} \leq |\gamma_{uv}| \leq \gamma_{B1} \quad \text{-----} \quad (3.19)$$

Substituting Eq.(3.19) into Eq.(3.17) and arranging it, then the following equivalent shear stress-strain relation is derived (see Fig. 10),

$$\begin{aligned} \tau_{uv,eq1} &= G_{eq1} (\gamma_{uv} - |\gamma_{y1}|) \quad , \quad \gamma_{y1} = 0.0436W/e \quad \text{-----} \quad (3.20) \\ G_{eq1} &= (0.141/W - 1.0) (1.526\sqrt{f_c} - 7.365)e \end{aligned}$$

where $G_{eq1} = 0$ for $-\gamma_{y1} \leq \gamma_{uv} \leq \gamma_{y1}$; $\tau_{uv,eq1}$: the equivalent shear stress(kg/cm^2) ; G_{eq1} : the equivalent shear stiffness(kg/cm^2) ; and γ_{y1} : the shear strain at which aggregate interlock becomes effective. The limit shear strain at which aggregate interlock disappears is assumed as follows on the basis of the experimental result[6],

$$\gamma_{B1} = (0.01799 + 4.1857W)/e \quad \text{----- (3.21)}$$

The equivalent shear stiffness of cracked concrete becomes maximum when crack just occurs and is roughly equal to 0.1 E.

Now, the equivalent shear stress in the local coordinates U,V defined in the above is converted into the stresses $\{\sigma_{x,eq1}, \sigma_{y,eq1}, \tau_{xy,eq1}\}^T$ in the global coordinates X,Y as follows,

$$\begin{Bmatrix} \sigma_{x,eq1} \\ \sigma_{y,eq1} \\ \tau_{xy,eq1} \end{Bmatrix} = \begin{bmatrix} \cos^2\theta_{cr} & \sin^2\theta_{cr} & -2\cos\theta_{cr}\sin\theta_{cr} \\ \sin^2\theta_{cr} & \cos^2\theta_{cr} & 2\cos\theta_{cr}\sin\theta_{cr} \\ \cos\theta_{cr}\sin\theta_{cr} & -\cos\theta_{cr}\sin\theta_{cr} & \cos^2\theta_{cr} - \sin^2\theta_{cr} \end{bmatrix} \begin{Bmatrix} 0 \\ 0 \\ \tau_{uv,eq1} \end{Bmatrix} \quad (3.23)$$

Fig.11 shows the reduction of shear modulus due to cracking which is evaluated from Eq.(3.20) and those which have been used by different investigators[7], and a discrepancy among them is considerable, ranging from about 40 to 3 percents for very wide cracks. Fig.12 shows a comparison between the equivalent shear stress-strain relation calculated from Eq.(3.20) and that observed by the experiment[6] for several crack widths and constant concrete strength.

3.5 Equivalent Shear Stiffness due to Dowel Action

Dulacscka[8] conducted the dowel test whose variable factors were concrete strength and diameter and angle of reinforcing bar, and he proposed the relative displacement-dowel force relation,

$$\delta_s = \Delta (358T_y/D\sqrt{f_c}) \times 10^{-6} \quad \text{----- (3.24)}$$

$$\Delta = (T/T_y) \sqrt{\tan[(T/T_y)(\pi/2)]} \quad \text{----- (3.25)}$$

$$T_y = 0.2D^2 \sigma_y \{ \sqrt{\rho^2 \sin^2 \theta_{cr} + \rho f_c / 0.03 \sigma_y} - \rho \sin \theta_{cr} \} \quad \text{----- (3.26)}$$

where $\rho = 1 - (\sigma_s/\sigma_y)^2$; T_y : the dowel strength of one reinforcing bar(kg); T : the dowel force(kg); σ_s : the steel stress(kg/cm²); σ_y : the yield stress of steel(kg/cm²); D : the diameter of reinforcing bar(cm); and θ_{cr} : the angle between the axis perpendicular to the crack direction and the reinforcing bar.

Δ in Eq.(3.25) is a function of the non-dimensional dowel force T/T_y and gives the curve as shown in Fig.13. This curve is approximated by the elastoplastic relation,

.for elastic case ; $T/T_y = \alpha \cdot \Delta \quad \text{----- (3.27)}$

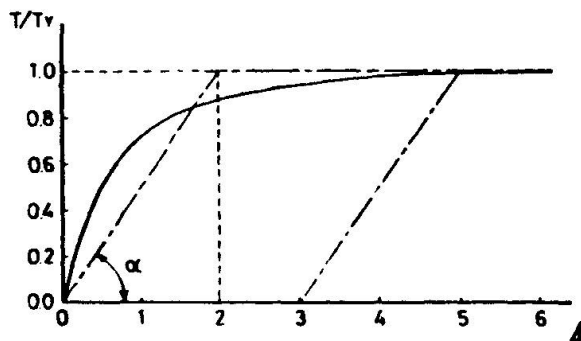


Fig.13 Non-Dimensionized Dowel Force Curve

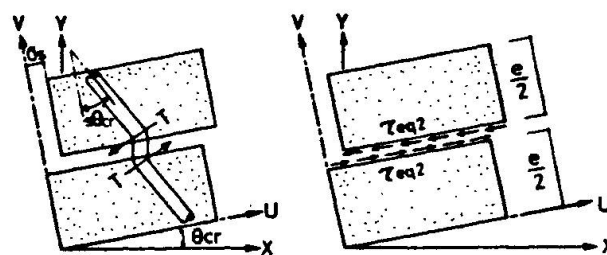


Fig.14 Idealization for Dowel Force



.for plastic case ;

$$T/T_y = 1.0 \text{ ---- (3.27)}$$

where α indicates the elastic slope and is set equal to 0.2.

In the next place, in order to evaluate the equivalent shear stiffness due to dowel action, the dowel force is replaced by the equivalent shear stress as shown in Fig.14,

$$\tau_{uv,eq2} = p_{\bar{x}} T \cos_s \theta_{cr} / s \text{ ---- (3.28)}$$

Substituting Eqs. (3.19), (3.27) and (3.28) into Eq. (3.24) and arranging it, then the following equivalent shear stress-strain relation is obtained,

.for elastic case ($|\gamma_{uv}| \leq \gamma_{y2}$) ;

$$\left. \begin{aligned} \tau_{uv,eq2} &= G_{eq2} \cdot \gamma_{uv} \\ G_{eq2} &= (\alpha \cdot D \sqrt{f_c} \cdot e \cdot p_{\bar{x}} \cos_s \theta_{cr}) \times 10^6 / 358 s A \end{aligned} \right\} \text{---- (3.29)}$$

.for plastic case ($|\gamma_{uv}| \geq \gamma_{y2}$) ;

$$\left. \begin{aligned} |\tau_{uv,eq2}| &= p_{\bar{x}} \cdot T_y \cos_s \theta_{cr} / s A \\ |\gamma_{y2}| &= 358 T_y \times 10^{-6} / \alpha \cdot D \sqrt{f_c} \cdot e \end{aligned} \right\} \text{---- (3.30)}$$

A transformation of the equivalent shear stress $\tau_{uv,eq2}$ in the U,V-coordinate system to that $(\sigma_{x,eq2}, \sigma_{y,eq2}, \tau_{xy,eq2})$ in the X,Y-coordinate system is to be done in the same way as Eq. (3.23). The relation between ratios G_{eq2}/G of equivalent shear stiffnesses G_{eq2} of Eq. (3.29) to the elastic shear stiffness G and angles $s\theta_{cr}$ of reinforcing bars is plotted in Fig.15 for several steel ratios, and it is found that an effect of dowel action is relatively small.

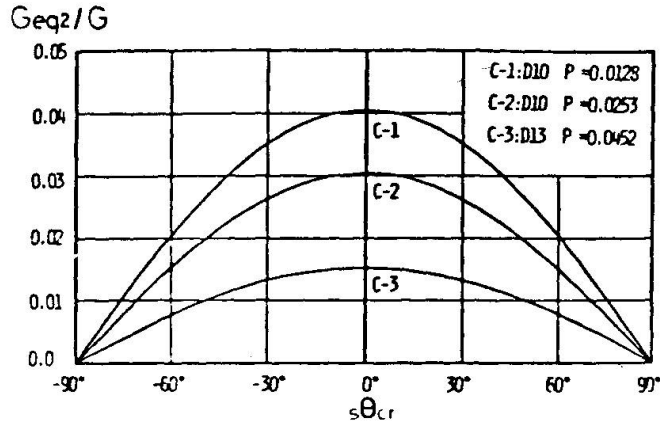


Fig.15 Equivalent Shear Stiffness due to Dowel Action

4. CRACK SPACING AND CRACK WIDTH

It is necessary for evaluating aggregate interlock and dowel action described in the previous section and also checking up the opening and closing of cracks in cyclic analysis to determine crack spacing and width.

Morita et al. [9] found from their own experiment that there was a linear relationship between average minimum crack spacing e_{min} and ratios D/p of bar diameters D to steel ratios p . Thus, assuming that when steel yields average crack spacing e_{av} becomes e_{min} , the equation predicting $e_{\bar{x},av}$ is proposed,

$$e_{\bar{x},av} = 0.1476 + 0.19 \cdot D/p_{\bar{x}} + 0.0023 / s \epsilon_{\bar{x}} \text{ ---- (4.1)}$$

where $e_{\bar{x},av}$ indicates average crack spacing in the reinforcing direction \bar{X} , and note that this is a nominal crack spacing for any one of cracked concrete element.

Fig.16 shows a comparison between crack spacings of the experiment [10, 11 and 12] and those calculated from Eq. (4.1) for several ratios D/p , and they have

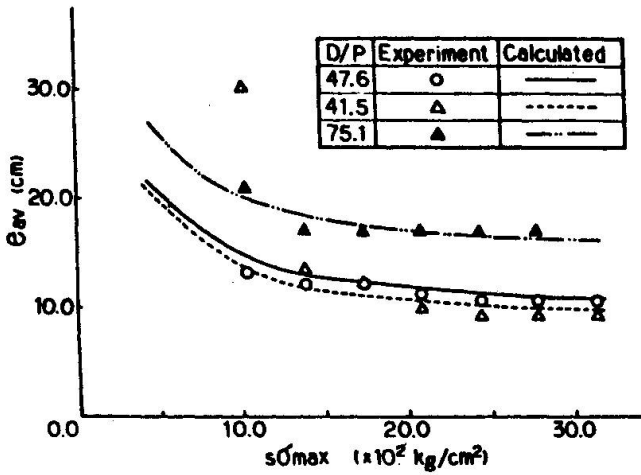


Fig.16 Comparison between Assumed and Observed Average Crack Spacing-Steel stress Relation

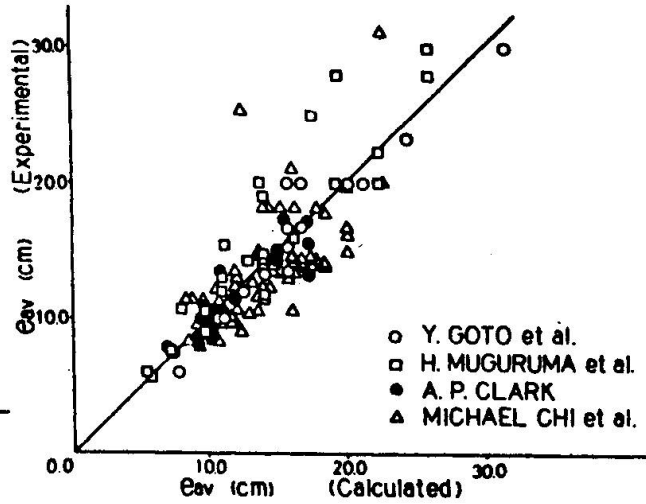


Fig.17 Comparison between Calculated and Experimental Crack Spacings

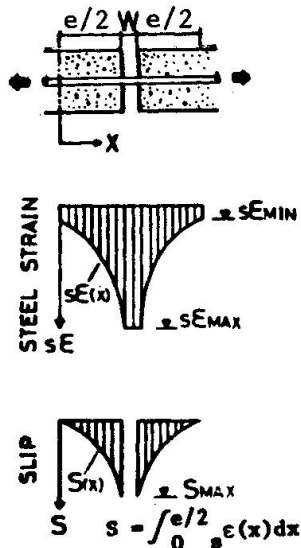


Fig.18 Distributions of Steel Strain and Slip along Reinforcing Bar in Cracked Concrete

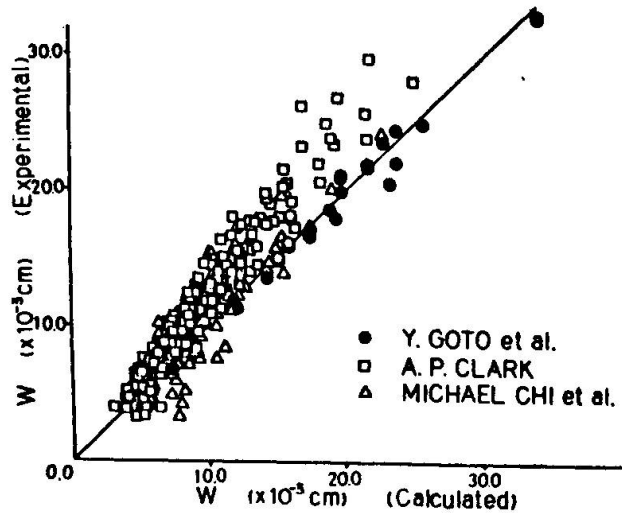


Fig.19 Comparison between Calculated and Experimental Crack Widths

some scatters at low stress levels but they fairly agree to each other with an increase of steel stresses.

Fig.17 shows plots of experimental crack spacings [9, 11, 12 and 13] against calculated values by Eq. (4.1) and it can be seen that although a discrepancy between them exists for big crack spacings, they coincide as crack spacings become smaller.

In the next place, a derivation of crack width based upon the conventional bond theory is presented. The slip increment ds over the interval dx is generally defined as a difference between elongations of concrete and reinforcing bar, and assuming that concrete strain after crack formation is negligible as compared with steel strain, then the slip is approximately expressed as follows,

$$S(x) = \int_0^x \epsilon_s(x) dx \quad \text{----- (4.2)}$$

The maximum slip is obtained from Eq. (4.2) as follows, provided that distributions of steel strain and slip over crack spacing e are given as shown in Fig.18,



$$S_{max} = \int_0^{e/2} s \epsilon(x) dx \quad \text{----- (4.3)}$$

Therefore, crack width W is defined as a function of maximum slip S_{max} and steel strain $s\epsilon_{max}$ at the cracking part,

$$W = 2.S_{max}(1 + s\epsilon_{max}) \quad \text{----- (4.4)}$$

However, it is hard to evaluate S_{max} since strain distribution of reinforcing bar along its length is unknown, so the average strain $s\epsilon_{\bar{x}}$ defined in Section 3.3 is adopted in this paper. But since strain at the cracking part is included in this average strain, it needs to redefine the net average strain excluding that strain,

$$s\epsilon_{\bar{x}}' = s\epsilon_{\bar{x}} - \frac{W}{\bar{x}}(s\epsilon_{max} - s\epsilon_{\bar{x}})/e \quad \text{----- (4.5)}$$

Thus, S_{max} is derived by using Eq.(4.5) instead of $s\epsilon(x)$ in Eq.(4.3) as follows,

$$S_{max} = e.s\epsilon_{\bar{x}}/2 - \frac{W}{\bar{x}}(s\epsilon_{max} - s\epsilon_{\bar{x}})/2 \quad \text{----- (4.6)}$$

An introduction of Eq.(4.6) into Eq.(4.4) results in the following crack width,

$$W_{\bar{x}} = e.s\epsilon_{\bar{x}}(1 + s\epsilon_{max}) / \{1 + (1 + s\epsilon_{max})(s\epsilon_{max} - s\epsilon_{\bar{x}})\} \quad \text{----- (4.7)}$$

where

$$s\epsilon_{max} = s\epsilon_{\bar{x}} + \sigma_{\bar{x},eq} / p_{\bar{x}} \cdot sE$$

Fig.19 shows plots of experimental crack widths observed in the tensile test (black circles)[13] and the flexural test of beams[11 and 12] against calculated values by Eq.(4.7).

Although the proposed equations for crack spacing and width give an evaluation on each reinforcing direction, it is useful from an analytical point of view to define crack spacings and widths normal to crack directions. Consider the general case in which concrete is reinforced in the orthogonal directions \bar{X}, \bar{Y} .

Letting $e_{\bar{x},av}, e_{\bar{y},av}, W_{\bar{x}}$ and $W_{\bar{y}}$ be average crack spacings and crack widths evaluated by Eq.(4.1) and (4.7), then the average crack spacing e_{av} perpendicular to the crack direction shall be either smaller one between the following two equations (see Fig.20),

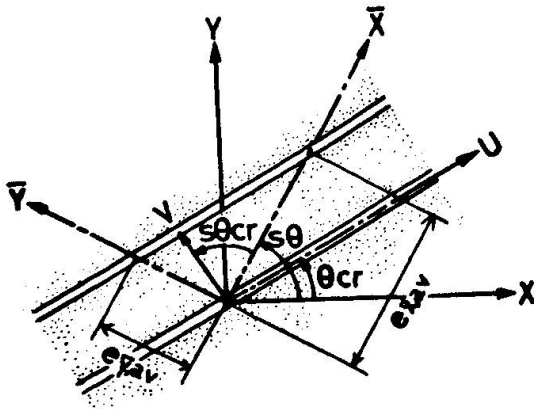


Fig.20 Representation of Crack Spacing

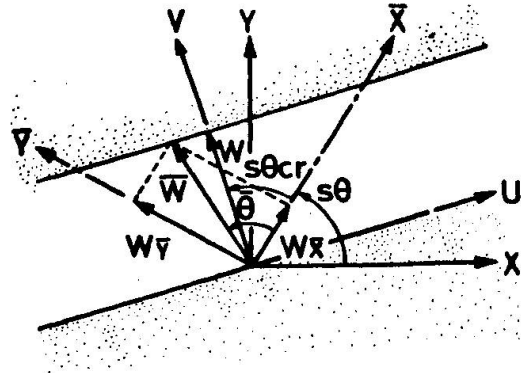


Fig.21 Representation of Crack Width

$$e_{av} = e_{\bar{x},av} \cos \theta_{s cr} \quad \text{or} \quad e_{av} = e_{\bar{y},av} \sin \theta_{s cr} \quad \text{----- (4.8)}$$

and crack width normal to the crack direction is given as follows(see Fig.21),

$$W = \bar{W} \cdot \cos(\bar{\theta} - \theta_{s cr}) \quad \text{----- (4.9)}$$

$$\bar{W} = \sqrt{W_{\bar{x}}^2 + W_{\bar{y}}^2}, \quad \bar{\theta} = \tan^{-1}(W_{\bar{y}}/W_{\bar{x}})$$

5. NUMERICAL PROCEDURE

5.1 Finite Element

In order to improve accuracy and reduce number of degrees of freedom, the composite element with four nodes and eight degrees of freedom is developed from four constant strain quadrilaterals with nine nodes and eighteen degrees of freedom through the conventional condensation process as shown in Fig.22 and we refer this to as the Super Element[14].

5.2 Solution Procedure

An incremental initial stress approach or an incremental self-correcting approach is used to solve governing nonlinear equations. However, the latter approach is suitable from a viewpoint of a stability and a computational time when cyclic behaviors are to be followed.

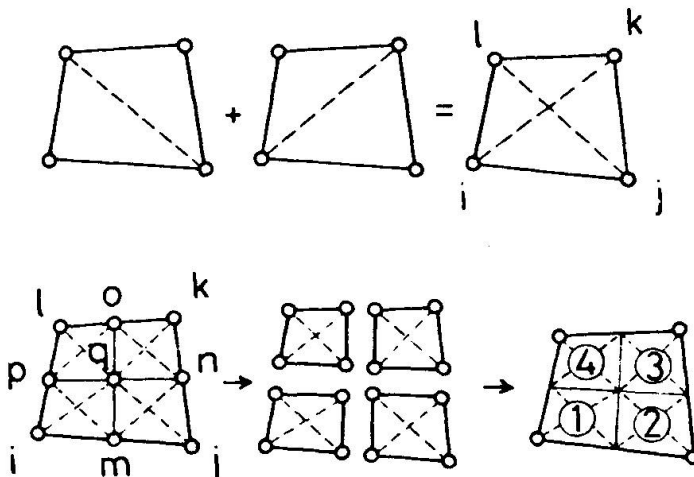
Now, the incremental self-correcting approach proposed by Stricklin et al.[15] in which a nonlinear analysis is performed by using the initial stiffness all over the computational process without iterations is briefly described. According to this approach, the incremental deflection $\Delta\{\delta\}$ is calculated from the following equations for materially nonlinear problems,

$$\Delta\{\delta\} = [K_0]^{-1}(\Delta P\{\bar{P}\} + \Delta\{Q_p\} + \Delta P \cdot Z \{f\}) \quad \text{----- (5.1)}$$

$$\{f\} = -[K_0]\{\delta\} + P\{\bar{P}\} + \{Q_p\} \quad \text{----- (5.2)}$$

where $\{f\}$: the force in unbalance induced by the deflection $\{\delta\}$ which does not satisfy equilibrium ; $[K_0]$: the initial stiffness ; $\{Q_p\}$: the fictitious load due to material nonlinearities ; P : the load parameter^P; $\{\bar{P}\}$: the normalized load vector ; Z : the correcting factor ; and ΔPZ is conventionally set equal to 1.2.

Fig.22 Composition of Super Element





REFERENCES

1. G.C.Nayak and O.C.Zienkiewicz, "Convenient Form of Stress Invariants for Plasticity," Proceedings of A.S.C.E., Vol.98, No.ST4, April 1972.
2. V.Cervenka and K.H.Gerstle, "Inelastic Analysis of Reinforced Concrete Panels, Part I ; Theory," IABSE Publications, Vol.31-II, 1971.
3. T.Sato and N.Shirai, "Analysis of Nonlinear Behaviors of Concrete by Finite Element Method," The Summary of the Joint Meetings of Applied Mechanics, No.25, 1975 (in Japanese).
4. S.Morita, "Study on Bond Effect of Reinforced Concrete Members by Tensile Tests," The Annual Report of Cement Engineering, Vol.XVII, 1963 (in Japanese).
5. S.Morita et al., "Study on Bond Effect of Reinforced Concrete Members by Tensile Tests," The Annual Report of Cement Engineering, Vol.XVIII, 1964 (in Japanese).
6. T.Paulay et al., "Mechanism of Shear Resistance of Concrete Beams," Proceedings of A.S.C.E., Vol.94, No.ST10, 1968.
7. K.H.Gerstle, "Material Modelling of Reinforced Concrete," Advanced Mechanics of Reinforced Concrete, Introductory Report, IABSE COLLOQUIUM DELFT 1981.
8. H.Dulacscka, "Dowel Action of Reinforcement Crossing Cracks in Concrete," Journal of ACI, 1972, pp.754 - 757.
9. S.Morita et al., "Control of Cracking in Reinforced Concrete Member," The 2nd Symposium on Deformed Bars, Concrete Library, No.14, 1965(in Japanese).
10. Edward G. Nawy, "Crack Control in Reinforced Concrete Structures," Journal of ACI, October 1968.
11. A.P.Clark, "Cracking in Reinforced Concrete Flexural Members," Journal of ACI, April 1956.
12. Michael Chi et al., "Flexural Cracks in Reinforced Concrete Beams," Journal of ACI, April, 1958.
13. Y.Goto et al., "Investigation on Tension Cracks in Reinforced Concrete Members - An Experiment by Tensile Bond Specimen-," The 2nd Symposium on Deformed Bars, Concrete Library, No.14, 1965 (in Japanese).
14. T.Sato and N.Shirai, "Inelastic Analysis of Reinforced Concrete Shear Walls under Combined Stresses," The Annual Report of Architectural Institute of Japan, 1977 (in Japanese).
15. J.A.Stricklin et al., "Self-Correcting Incremental Approach in Nonlinear Structural Mechanics," Journal of AIAA, Vol.9, no.12, 1971.